



GOBIERNO
DE ESPAÑA

MINISTERIO
DE CIENCIA, INNOVACIÓN
Y UNIVERSIDADES



GENERALITAT
VALENCIANA

Conselleria de Innovación,
Universidades, Ciencia
y Sociedad Digital

Based on *JHEP* 10 (2022) 144
in collaboration with E. Akhmedov

A solar electron antineutrino flux from neutrino magnetic moments

Pablo Martínez-Miravé
IFIC (CSIC – Univ. València)
CERN Neutrino Platform Pheno Week 2023



IFIC
INSTITUT DE FÍSICA
CORPUSCULAR



UNIVERSITAT
DE VALÈNCIA



CSIC
Consejo Superior de Investigaciones Científicas

ASTROPARTICLES
Astroparticles and High Energy Physics Group



A solar electron antineutrino flux from neutrino magnetic moments

For Majorana neutrinos, the interaction of transition magnetic dipole moments with the solar magnetic field would give rise to a potentially detectable flux of solar antineutrinos on Earth.

NEUTRINO MAGNETIC MOMENTS

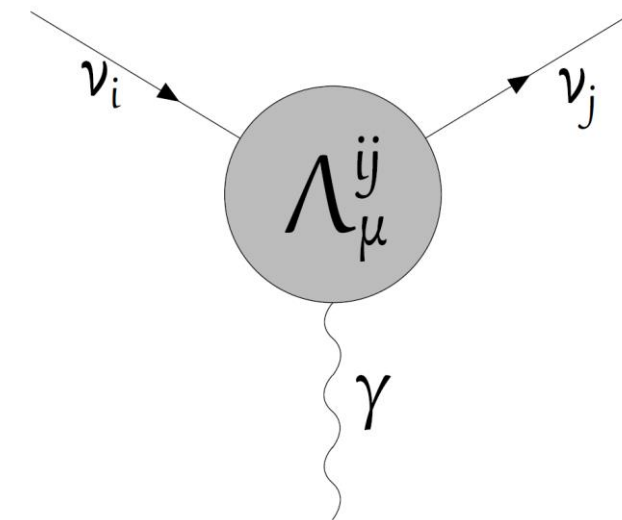
Neutrino magnetic dipole moments arise in many extensions of the Standard Model extensions through **quantum loops effects** which allow for:

- direct interactions of neutrinos with electromagnetic fields and
- electromagnetic interactions of neutrinos with charged particles.

Effectively,

$$\mathcal{L}_{\text{eff}} \propto \mu_{ij} \bar{\psi}_i \sigma_{\mu\nu} \psi_j F^{\mu\nu}$$

CHIRALITY-FLIPPING INTERACTION



MAJORANA NEUTRINOS and SPIN-FLAVOUR PRECESSION (SFP)

In the presence of an external magnetic field, neutrinos can simultaneously undergo a flip of chirality and a flavour transformation.

SPIN-FLAVOUR PRECESSION (SFP)

Phys. Lett. B 553 (2003) 7
Phys. Rev. D 97 (2018) 093006
and references therein

The process can be resonantly enhanced in matter

RESONANT SPIN-FLAVOUR PRECESSION (RSFP)

Phys. Rev. D 37 (1988) 1368
Phys. Lett. B 213 (1988) 64

MAJORANA NEUTRINOS and SPIN-FLAVOUR PRECESSION (SFP)

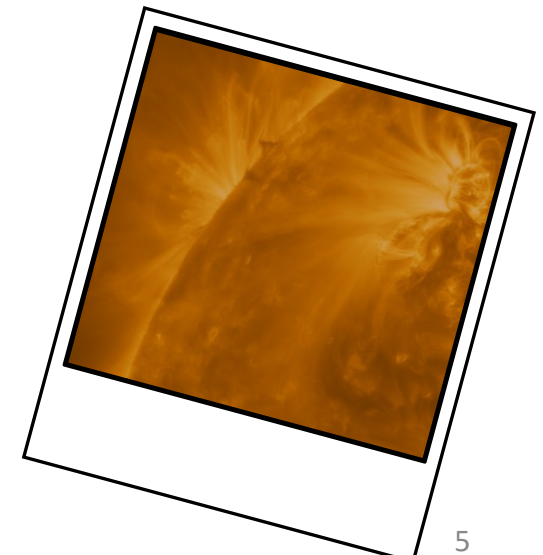
Astrophysical sources, in which large magnetic fields could be present, are ideal to probe spin-flavour precession.

Solar neutrino data is compatible with no SFP.

However, the effect of SFP could still be present at a subleading level.

How do we look for it?

- Search for a missing flux of neutrinos
- Search for a flux of antineutrinos



A SOLAR ELECTRON ANTINEUTRINO FLUX

We are interested in a flux of electron antineutrinos. Why?

Because that is what we can measure and distinguish.

$$\bar{\nu}_e + p \rightarrow e^+ + n$$

How do we get a flux of solar electron antineutrinos?

- Direct $\nu_{eL} \rightarrow \bar{\nu}_{eR}$ conversion is not possible for Majorana neutrinos
(CPT: $\mu_{\alpha\alpha} = 0$)
- Combination of spin-flavour precession and flavour conversion

$$\nu_{eL} \xrightarrow{\text{osc.}} \nu_{\mu L} \xrightarrow{\text{SFP}} \bar{\nu}_{eR}$$

$$\nu_{eL} \xrightarrow{\text{SFP}} \bar{\nu}_{\mu R} \xrightarrow{\text{osc.}} \bar{\nu}_{eR}$$

A SOLAR ELECTRON ANTINEUTRINO FLUX

- Combination of spin-flavour precession and flavour transformations

$$\nu_{eL} \xrightarrow{\text{osc.}} \nu_{\mu L} \xrightarrow{\text{SFP}} \bar{\nu}_{eR}$$

$$\nu_{eL} \xrightarrow{\text{SFP}} \bar{\nu}_{\mu R} \xrightarrow{\text{osc.}} \bar{\nu}_{eR}$$

Sov. Phys. JETP 68 (1989) 690
Phys. Rev. D 48 (1993) 2167

In the Sun, the amplitudes of the processes cancel almost exactly, so the only option left is

spin-flavour precession in the Sun

+

flavour conversion while travelling to Earth

A SOLAR ELECTRON ANTINEUTRINO FLUX

STATUS:

- Analytical (perturbative) calculation in a two-neutrino framework
[\(Akhmedov and Pulido, 2002\)](#)
- Expression for $P(\nu_{eL} \rightarrow \bar{\nu}_{eR})$ is used by **KamLAND**, **Borexino** and **Super-Kamiokande** to derive bounds on μB .

[Astrophys. J. 925 \(2022\) 14](#)
[Astropart. Phys. 125 \(2021\) 102509](#)
[Astropart. Phys. 139 \(2022\) 102702](#)

We extended the analysis to include 3-neutrino effects with updated solar models and revisited the existing experimental bounds.

A SOLAR ELECTRON ANTINEUTRINO FLUX

We extended the analysis to include 3-neutrino effects with updated solar models and revisited the existing experimental bounds.

KEY ASPECTS:

with 2 neutrino families only, there is only one non-zero magnetic moment

with 3 families, there are 3 non-zero magnetic moments.
Then, what are we constraining?

A SOLAR ELECTRON ANTINEUTRINO FLUX

We computed the electron antineutrino appearance probability

I. ANALYTICALLY:

- In a rotated basis (which simplifies the calculations) $\mu_{e'\mu'}, \mu_{e'\tau'}, \mu_{\mu'\tau'}$
- Assuming $\Delta m_{21}^2 \ll \Delta m_{31}^2$
- Perturbatively in μB (leading order)
- Assume all neutrinos are produced at one point
- Non-twisting magnetic field

II. NUMERICALLY:

- Including extended production regions
- Solving full evolution equations for linearly decreasing B

ELECTRON ANTINEUTRINO APPEARANCE PROBABILITY

The electron antineutrino appearance probability for three non-zero magnetic moments

$$P(\nu_{eL} \rightarrow \bar{\nu}_{eR}) = \frac{1}{2} c_{13}^2 \sin^2 2\theta_{12} B_\perp^2(r_0) \left[c_{13}^2 |\mu_{e'\mu'}|^2 \left(\frac{\cos^2 \tilde{\theta}(r_0)}{g'_1(r_0)} + \frac{\sin^2 \tilde{\theta}(r_0)}{g'_2(r_0)} \right)^2 \right. \\ \left. + \left(\frac{s_{13} |\mu_{\mu'\tau'}|}{2\Delta} \right)^2 - 2\text{Re}\{\mu_{e'\mu'}^* \mu_{\mu'\tau'}\} \left(\frac{\cos^2 \tilde{\theta}(r_0)}{g'_1(r_0)} + \frac{\sin^2 \tilde{\theta}(r_0)}{g'_2(r_0)} \right) \frac{s_{13} c_{13}}{2\Delta} \right] \\ + s_{13}^2 B_\perp^2(r_0) \left(\frac{c_{13} |\mu_{e'\tau'}|}{2\Delta} \right)^2,$$

ELECTRON ANTINEUTRINO APPEARANCE PROBABILITY

The electron antineutrino appearance probability for three non-zero magnetic moments

$$P(\nu_{eL} \rightarrow \bar{\nu}_{eR}) = \frac{1}{2} c_{13}^2 \sin^2 2\theta_{12} B_\perp^2(r_0) \left[c_{13}^2 |\mu_{e'\mu'}|^2 \left(\frac{\cos^2 \tilde{\theta}(r_0)}{g'_1(r_0)} + \frac{\sin^2 \tilde{\theta}(r_0)}{g'_2(r_0)} \right)^2 \right. \\ \left. + \left(\frac{s_{13} |\mu_{\mu'\tau'}|}{2\Delta} \right)^2 - 2 \text{Re} \{ \mu_{e'\mu'}^* \mu_{\mu'\tau'} \} \left(\frac{\cos^2 \tilde{\theta}(r_0)}{g'_1(r_0)} + \frac{\sin^2 \tilde{\theta}(r_0)}{g'_2(r_0)} \right) \frac{s_{13} c_{13}}{2\Delta} \right] \\ + s_{13}^2 B_\perp^2(r_0) \left(\frac{c_{13} |\mu_{e'\tau'}|}{2\Delta} \right)^2 ,$$

ELECTRON ANTINEUTRINO APPEARANCE PROBABILITY

The electron antineutrino appearance probability for three non-zero magnetic moments

$$P(\nu_{eL} \rightarrow \bar{\nu}_{eR}) = \frac{1}{2} c_{13}^2 \sin^2 2\theta_{12} B_\perp^2(r_0) \left[c_{13}^2 |\mu_{e'\mu'}|^2 \left(\frac{\cos^2 \tilde{\theta}(r_0)}{g'_1(r_0)} + \frac{\sin^2 \tilde{\theta}(r_0)}{g'_2(r_0)} \right)^2 \right. \\ \left. + \left(\frac{s_{13} |\mu_{\mu'\tau'}|}{2\Delta} \right)^2 - 2 \text{Re} \{ \mu_{e'\mu'}^* \mu_{\mu'\tau'} \} \left(\frac{\cos^2 \tilde{\theta}(r_0)}{g'_1(r_0)} + \frac{\sin^2 \tilde{\theta}(r_0)}{g'_2(r_0)} \right) \frac{s_{13} c_{13}}{2\Delta} \right] \\ + s_{13}^2 B_\perp^2(r_0) \left(\frac{c_{13} |\mu_{e'\tau'}|}{2\Delta} \right)^2 ,$$

ELECTRON ANTINEUTRINO APPEARANCE PROBABILITY

The electron antineutrino appearance probability for three non-zero magnetic moments

$$P(\nu_{eL} \rightarrow \bar{\nu}_{eR}) = \frac{1}{2} c_{13}^2 \sin^2 2\theta_{12} B_\perp^2(r_0) \left[c_{13}^2 |\mu_{e'\mu'}|^2 \left(\frac{\cos^2 \tilde{\theta}(r_0)}{g'_1(r_0)} + \frac{\sin^2 \tilde{\theta}(r_0)}{g'_2(r_0)} \right)^2 \right.$$

$$\left. + \left(\frac{s_{13} |\mu_{\mu'\tau'}|}{2\Delta} \right)^2 - 2\text{Re}\{\mu_{e'\mu'}^* \mu_{\mu'\tau'}\} \left(\frac{\cos^2 \tilde{\theta}(r_0)}{g'_1(r_0)} + \frac{\sin^2 \tilde{\theta}(r_0)}{g'_2(r_0)} \right) \frac{s_{13} c_{13}}{2\Delta} \right]$$

r_0 is the production point in the Sun

$\tilde{\theta}$ is the effective mixing angle

$g_{1,2}(r)$ depend on the neutrino energy and matter potentials

$$+ s_{13}^2 B_\perp^2(r_0) \left(\frac{c_{13} |\mu_{e'\tau'}|}{2\Delta} \right)^2,$$



THE ROLE OF EACH MAGNETIC MOMENT

The electron antineutrino appearance probability for three non-zero magnetic moments

$$P(\nu_{eL} \rightarrow \bar{\nu}_{eR}) = \frac{1}{2} c_{13}^2 \sin^2 2\theta_{12} B_\perp^2(r_0) \left[c_{13}^2 |\mu_{e'\mu'}|^2 \left(\frac{\cos^2 \tilde{\theta}(r_0)}{g'_1(r_0)} + \frac{\sin^2 \tilde{\theta}(r_0)}{g'_2(r_0)} \right)^2 \right.$$
$$\left. + \left(\frac{s_{13} |\mu_{\mu'\tau'}|}{2\Delta} \right)^2 - 2\text{Re}\{\mu_{e'\mu'}^* \mu_{\mu'\tau'}\} \left(\frac{\cos^2 \tilde{\theta}(r_0)}{g'_1(r_0)} + \frac{\sin^2 \tilde{\theta}(r_0)}{g'_2(r_0)} \right) \frac{s_{13} c_{13}}{2\Delta} \right]$$
$$\Delta = \frac{\Delta m_{31}^2}{4E}$$

Some contributions are suppressed by the smallness of the reactor mixing angle.

$$+ s_{13}^2 B_\perp^2(r_0) \left(\frac{c_{13} |\mu_{e'\tau'}|}{2\Delta} \right)^2,$$



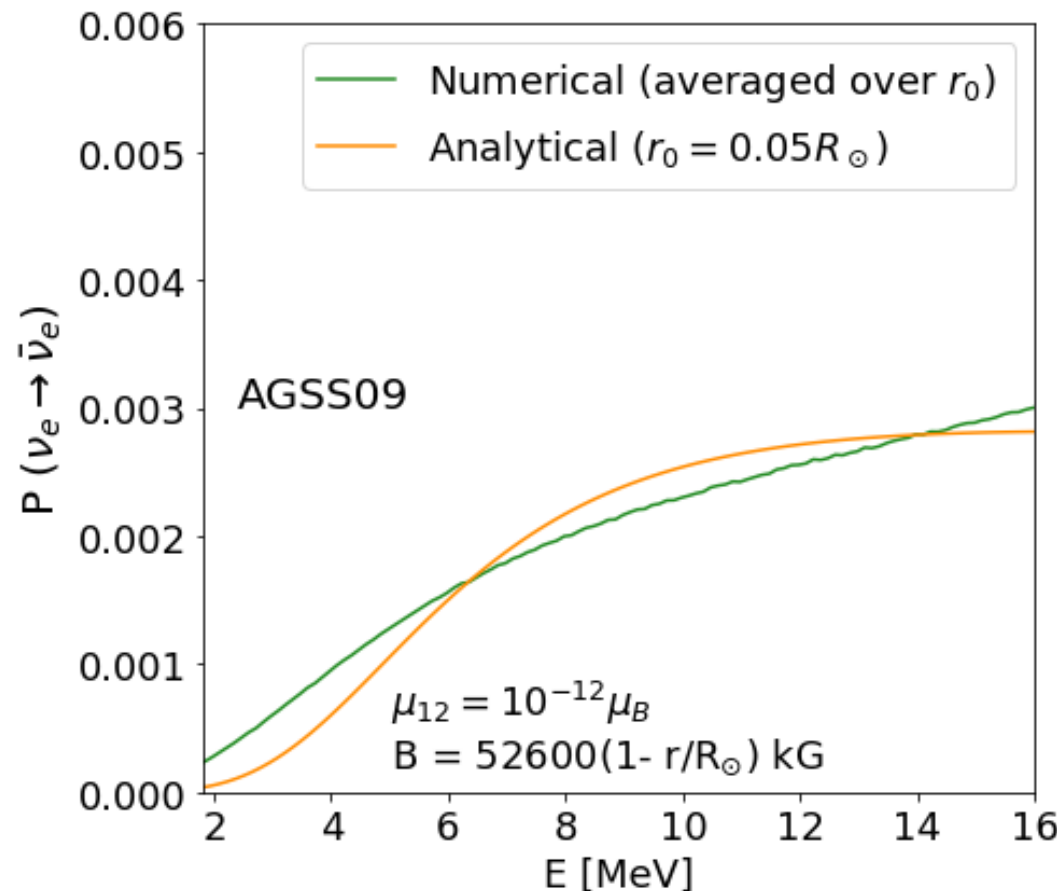
THE ROLE OF EACH MAGNETIC MOMENT

The electron antineutrino appearance probability for three non-zero magnetic moments

$$P(\nu_{eL} \rightarrow \bar{\nu}_{eR}) = \frac{1}{2} c_{13}^2 \sin^2 2\theta_{12} B_\perp^2(r_0) \left[c_{13}^2 |\mu_{e'\mu'}|^2 \left(\frac{\cos^2 \tilde{\theta}(r_0)}{g'_1(r_0)} + \frac{\sin^2 \tilde{\theta}(r_0)}{g'_2(r_0)} \right)^2 \right.$$
$$+ \left(\frac{s_{13} |\mu_{\mu'\tau'}|}{2\Delta} \right)^2 - 2\text{Re}\{\mu_{e'\mu'}^* \mu_{\mu'\tau'}\} \left(\frac{\cos^2 \tilde{\theta}(r_0)}{g'_1(r_0)} + \frac{\sin^2 \tilde{\theta}(r_0)}{g'_2(r_0)} \right) \frac{s_{13} c_{13}}{2\Delta} \left. \right]$$
$$+ s_{13}^2 B_\perp^2(r_0) \left(\frac{c_{13} |\mu_{e'\tau'}|}{2\Delta} \right)^2,$$

ELECTRON ANTINEUTRINO APPEARANCE PROBABILITY

Comparison with the numerical results shows a **good agreement** for ${}^8\text{B}$ neutrinos



Discrepancies at low energies,
but in that region, the probability
is much smaller



THE ROLE OF EACH MAGNETIC MOMENT

The electron antineutrino appearance probability for three non-zero magnetic moments

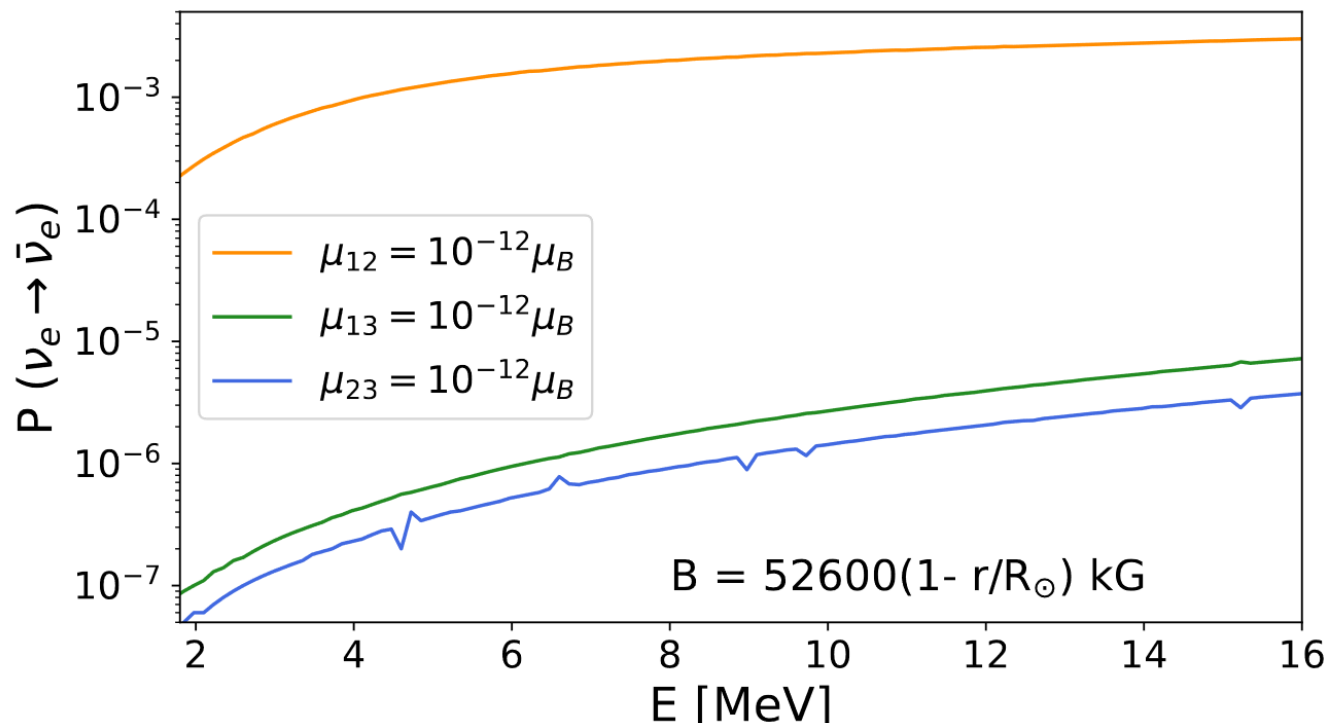
$$P(\nu_{eL} \rightarrow \bar{\nu}_{eR}) = \frac{1}{2} c_{13}^2 \sin^2 2\theta_{12} B_\perp^2(r_0) \left[c_{13}^2 |\mu_{e'\mu'}|^2 \left(\frac{\cos^2 \tilde{\theta}(r_0)}{g'_1(r_0)} + \frac{\sin^2 \tilde{\theta}(r_0)}{g'_2(r_0)} \right)^2 \right.$$
$$\left. + \left(\frac{s_{13} |\mu_{\mu'\tau'}|}{2\Delta} \right)^2 - 2\text{Re}\{\mu_{e'\mu'}^* \mu_{\mu'\tau'}\} \left(\frac{\cos^2 \tilde{\theta}(r_0)}{g'_1(r_0)} + \frac{\sin^2 \tilde{\theta}(r_0)}{g'_2(r_0)} \right) \frac{s_{13} c_{13}}{2\Delta} \right]$$
$$+ s_{13}^2 B_\perp^2(r_0) \left(\frac{c_{13} |\mu_{e'\tau'}|}{2\Delta} \right)^2,$$

Some contributions are suppressed by the smallness of the reactor mixing angle.

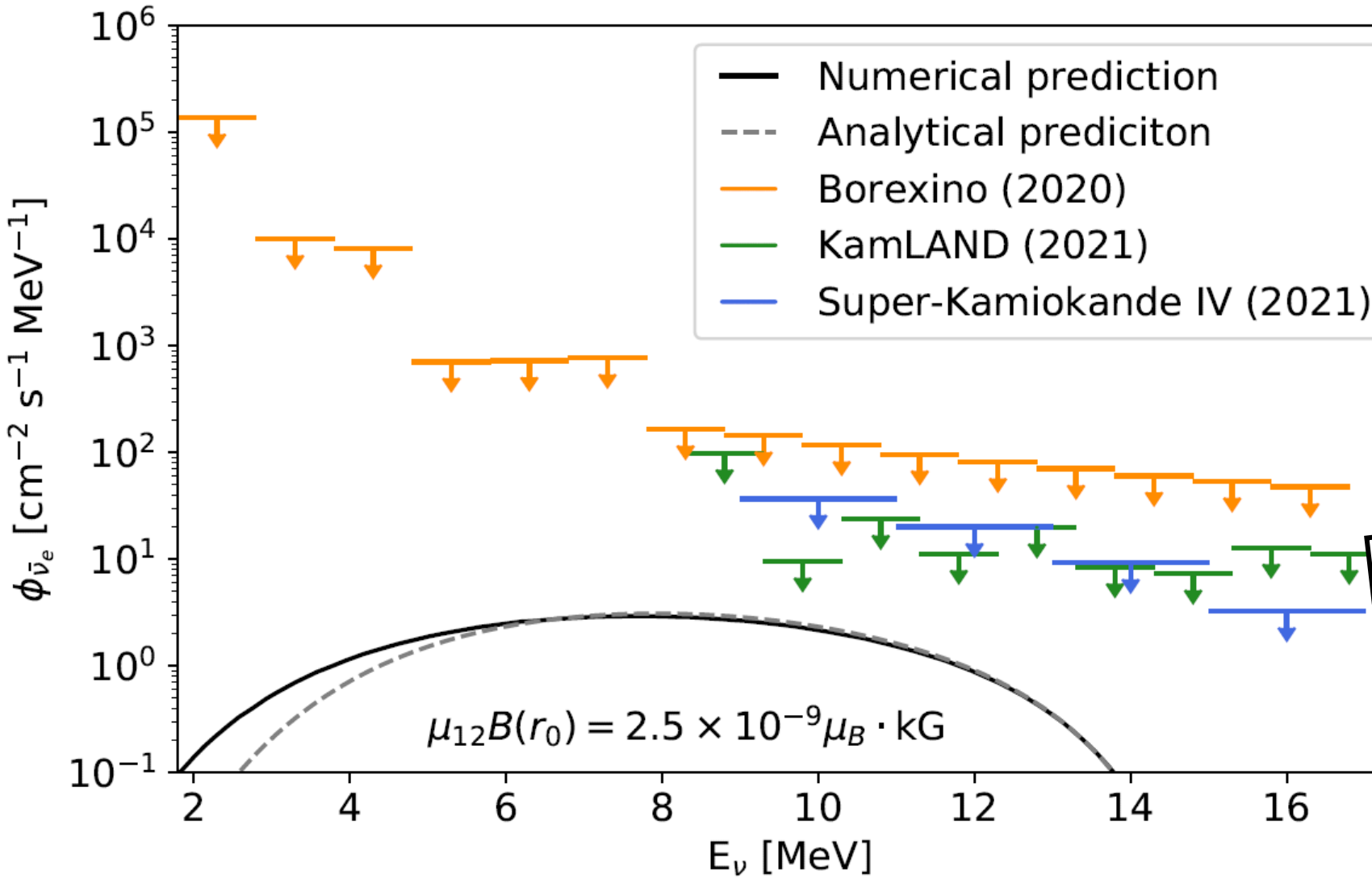


THE ROLE OF EACH MAGNETIC MOMENT

Assuming **only one non-zero magnetic moment at a time**, we confirm numerically that the main contribution is due to μ_{12} .



REVISITING EXISTING LIMITS

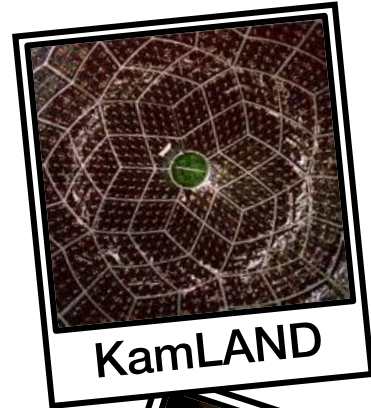


REVISITING EXISTING LIMITS

KamLAND:

$$(\mu_{12}B_{\perp}(r_0))_{\text{AGSS09}} < (4.9 - 5.1) \times 10^{-9} \mu_B \text{ kG}$$

$$(\mu_{12}B_{\perp}(r_0))_{\text{GS98}} < (4.7 - 4.8) \times 10^{-9} \mu_B \text{ kG}$$

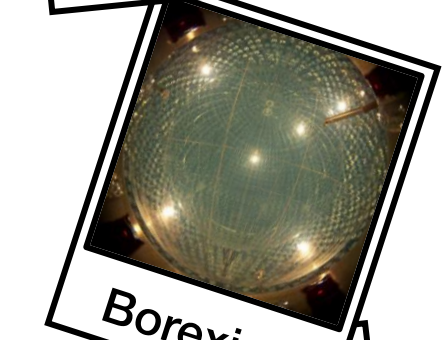


KamLAND

Borexino:

$$(\mu_{12}B_{\perp}(r_0))_{\text{AGSS09}} < (1.8 - 1.9) \times 10^{-8} \mu_B \text{ kG}$$

$$(\mu_{12}B_{\perp}(r_0))_{\text{GS98}} < (1.7 - 1.8) \times 10^{-8} \mu_B \text{ kG}$$

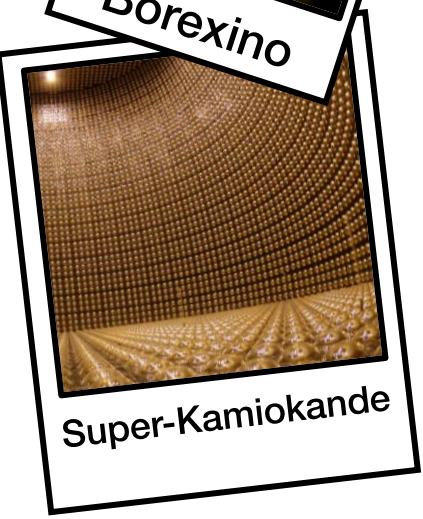


Borexino

Super-Kamiokande:

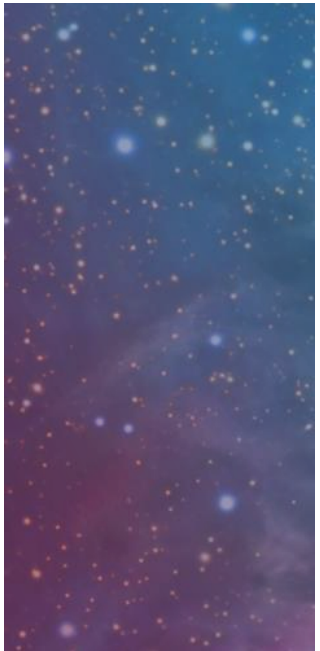
$$(\mu_{12}B_{\perp}(r_0))_{\text{AGSS09}} < (7.1 - 7.3) \times 10^{-9} \mu_B \text{ kG}$$

$$(\mu_{12}B_{\perp}(r_0))_{\text{GS98}} < (6.8 - 6.9) \times 10^{-9} \mu_B \text{ kG}$$



Super-Kamiokande

INTERPRETING LIMITS



Pressure of the magnetic field in the solar core does not exceed matter pressure Nucl. Phys. B Proc. Suppl. 35 (1994) 321

$$B < 10^9 \text{ G} \quad \longrightarrow \quad \mu_{12} < 5 \times 10^{-15} \mu_B$$

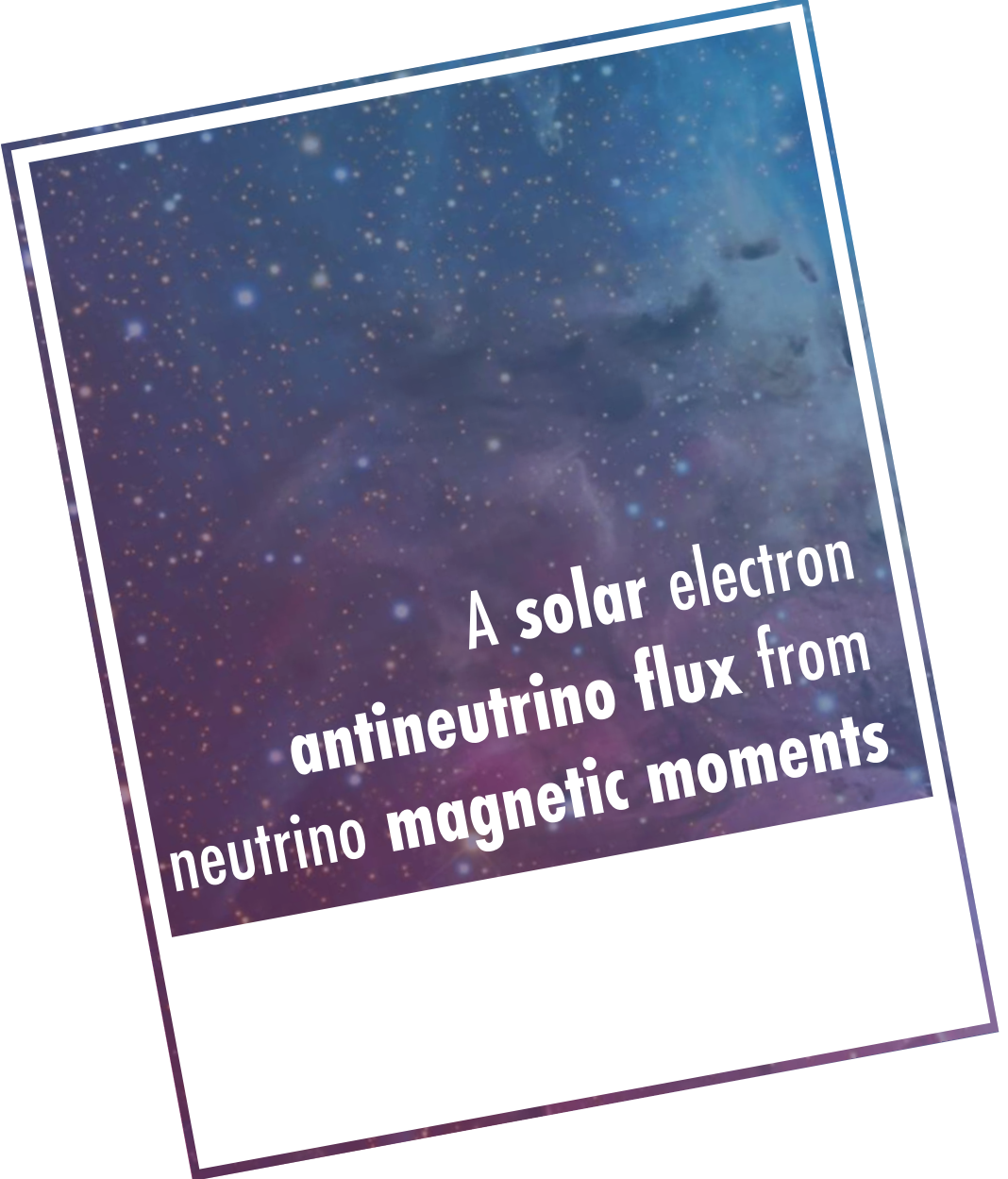
Stability of toroidal magnetic fields in the radiative zone of the Sun
Astronomy Reports 52 (2011) 247

$$B \lesssim 600 \text{ G} \quad \longrightarrow \quad \mu_{12} < 8.3 \times 10^{-9} \mu_B$$

Assume limit from XENONnT, LZ, PANDAX apply directly to μ_{12}

$$B_\perp < 1 \text{ MG} \quad \longleftarrow \quad \mu_\nu$$





A solar electron
antineutrino flux from
neutrino magnetic moments

For Majorana neutrinos, the interaction of transition magnetic dipole moments with the solar magnetic field would give rise to a potentially detectable flux of solar antineutrinos on Earth.



GRÀCIES
THANK YOU
GRACIAS



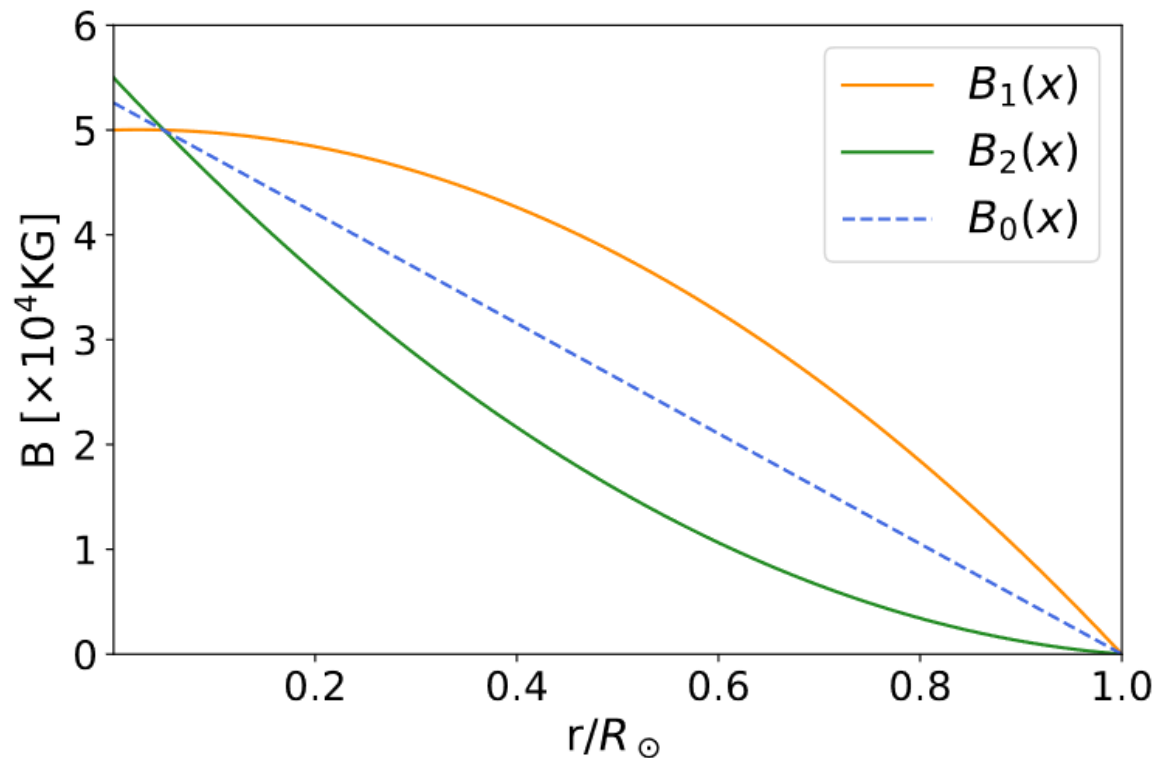


SPARE SLIDES



THE ROLE OF THE MAGNETIC FIELD PROFILE

We studied the difference expected by parameterising the magnetic field inside the Sun in three different ways, with the same strength at the main production point (one linear and two quadratic).



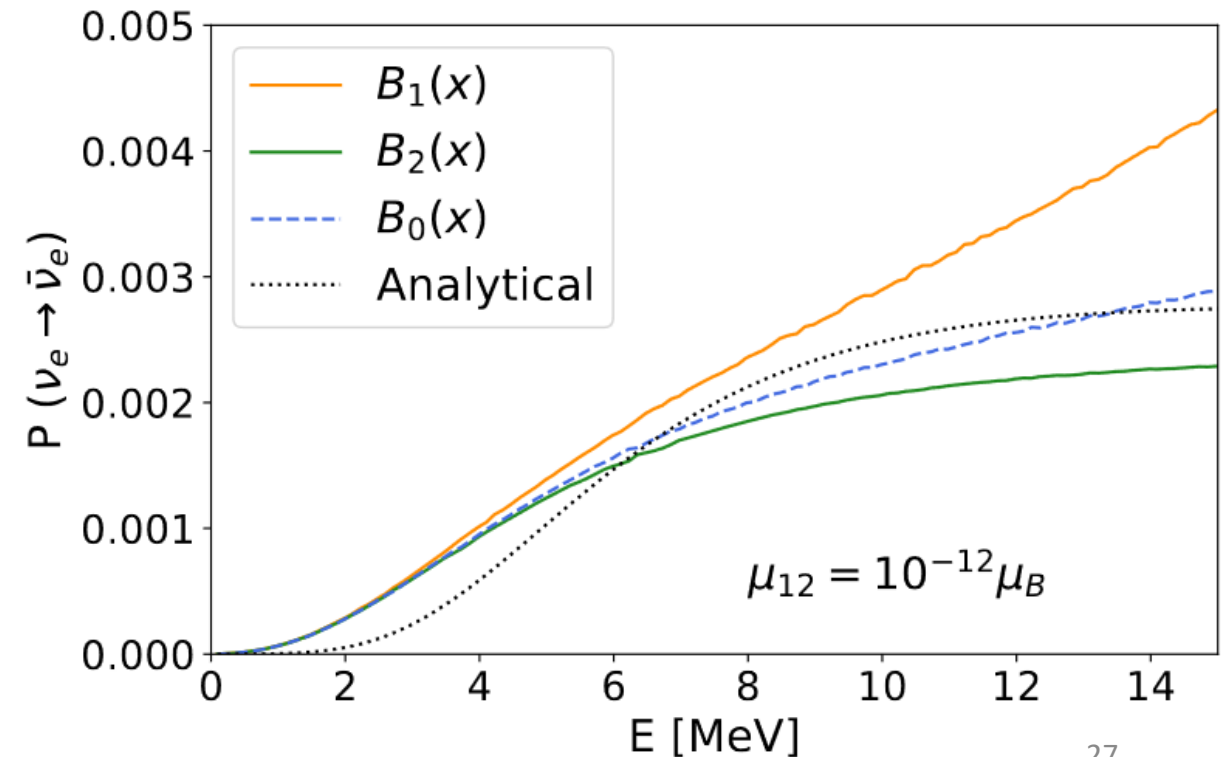
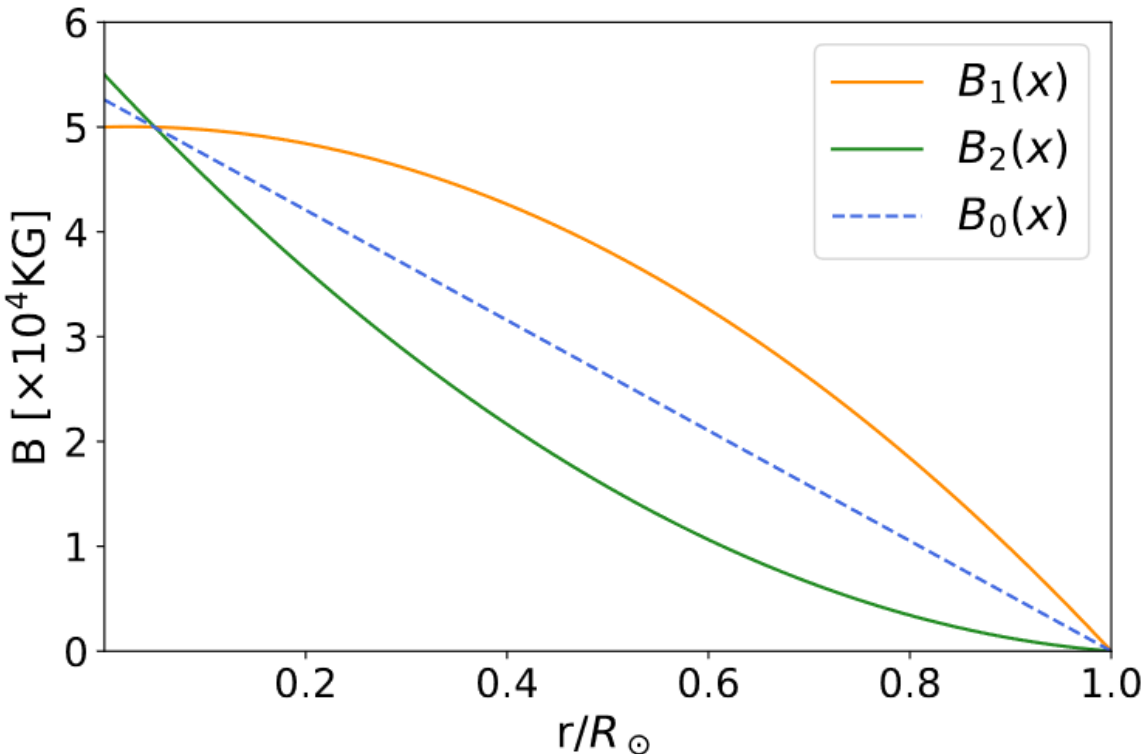
$$B_1(r) = 50000 + 2632 \frac{r}{R_\odot} - 52632 \left(\frac{r}{R_\odot} \right)^2 \text{ kG}$$

$$B_2(r) = 55000 - 102368 \frac{r}{R_\odot} + 47368 \left(\frac{r}{R_\odot} \right)^2 \text{ kG}$$



THE ROLE OF THE MAGNETIC FIELD PROFILE

A larger sensitivity to the magnetic field profile is expected at [higher energies](#).



REVISITING EXISTING LIMITS

KamLAND:

$$(\mu_{12}B_{\perp}(r_0))_{\text{AGSS09}} < (4.9 - 5.1) \times 10^{-9} \mu_B \text{ kG}$$

$$(\mu_{12}B_{\perp}(r_0))_{\text{GS98}} < (4.7 - 4.8) \times 10^{-9} \mu_B \text{ kG}$$



Borexino:

$$(\mu_{12}B_{\perp}(r_0))_{\text{AGSS09}} < (1.8 - 1.9) \times 10^{-8} \mu_B \text{ kG}$$

$$(\mu_{12}B_{\perp}(r_0))_{\text{GS98}} < (1.7 - 1.8) \times 10^{-8} \mu_B \text{ kG}$$

Super-Kamiokande:

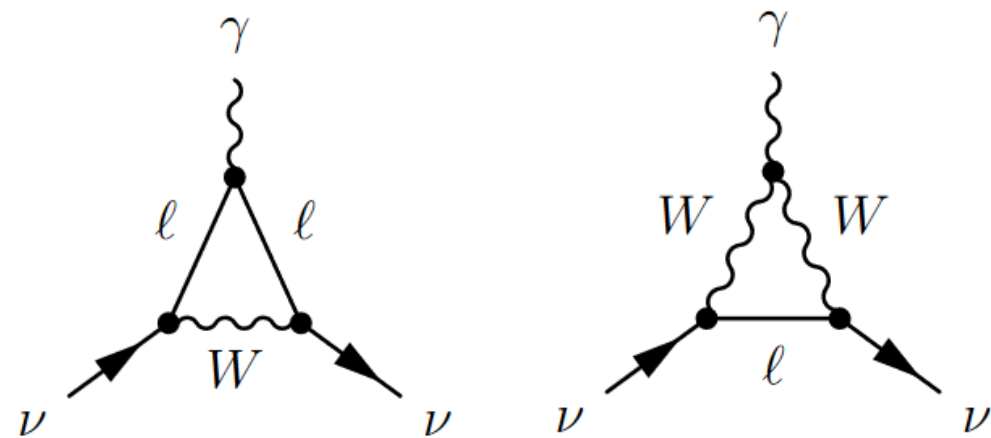
$$(\mu_{12}B_{\perp}(r_0))_{\text{AGSS09}} < (7.1 - 7.3) \times 10^{-9} \mu_B \text{ kG}$$

$$(\mu_{12}B_{\perp}(r_0))_{\text{GS98}} < (6.8 - 6.9) \times 10^{-9} \mu_B \text{ kG}$$

A yellow exclamation mark inside a yellow-bordered box with the text "Discrepancies in a factor 2-2.6 due to unsuitable approximation for their energy range".



NEUTRINO MAGNETIC MOMENTS



In the simplest SM extension with right-handed neutrinos:

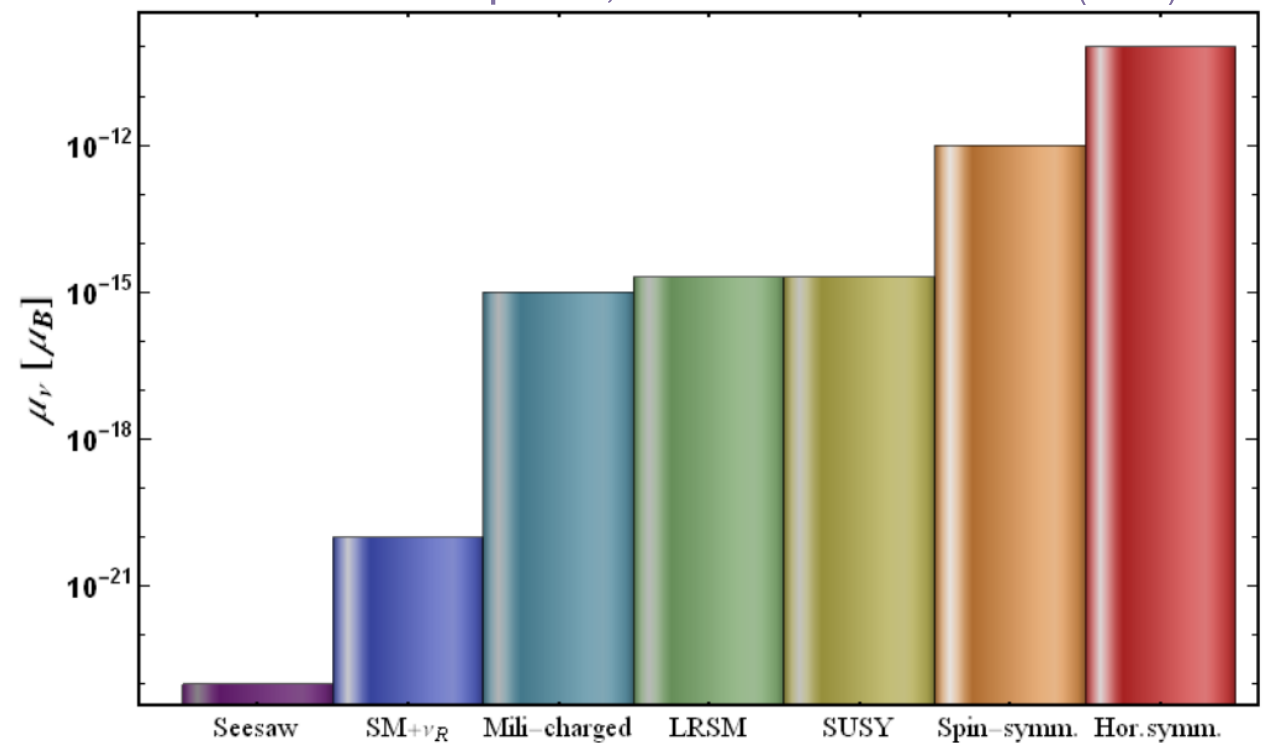
$$\mu_\nu^{ij} \leq \frac{3eG_F}{8\sqrt{2}\pi^2} m_\nu = 3 \times 10^{-20} \mu_B \left(\frac{m_\nu}{10^{-1} \text{ eV}} \right)$$

NEUTRINO MAGNETIC MOMENTS

Large magnetic moments are predicted in different extensions of the SM, among which **left-right symmetric models or SUSY**.

If a non-zero magnetic moment was observed, it would be a clear indication of **BSM physics**.
Also different depending on **Dirac or Majorana nature of neutrinos!**

Sudip Jana, PoS DISCRETE2020-2021 (2022) 037

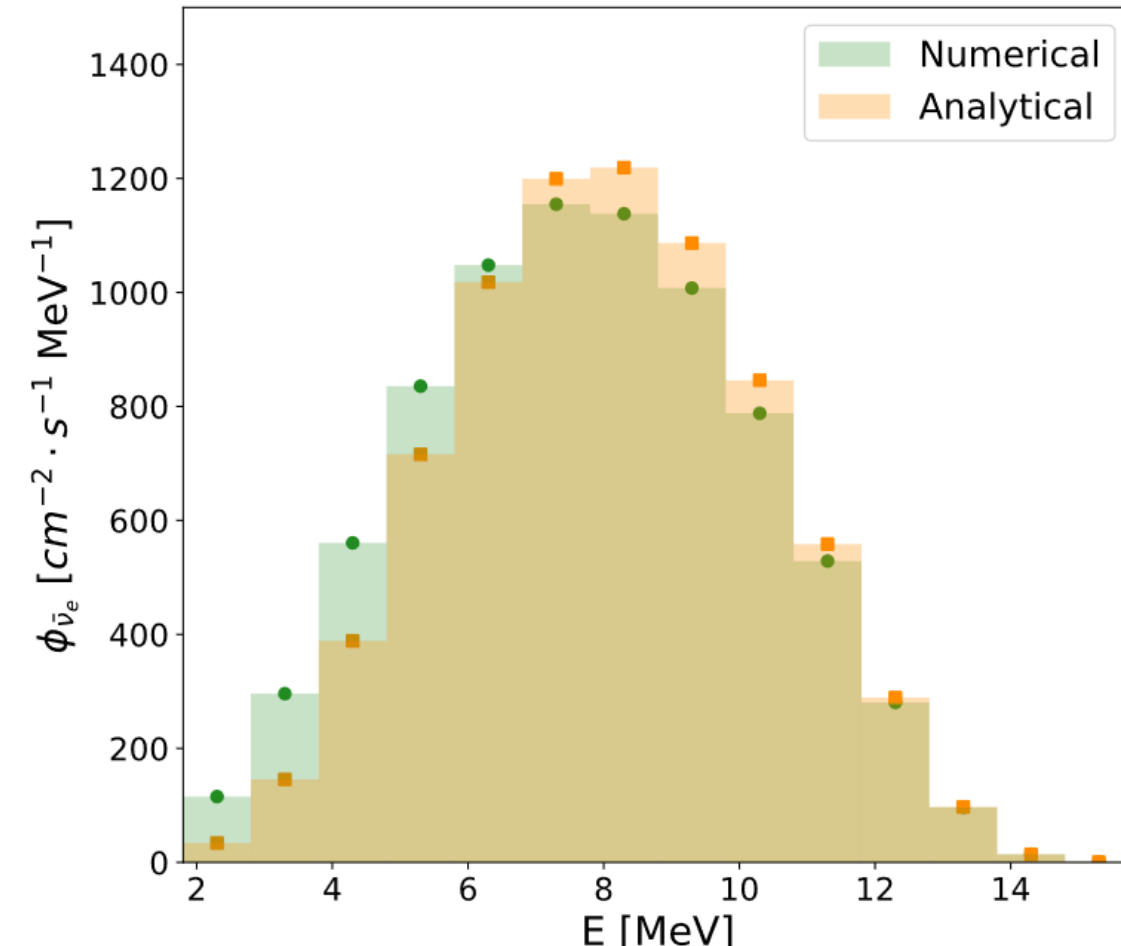


USEFUL INFORMATION FOR FUTURE SEARCHES

Experiments usually constrain the flux of astrophysical antineutrinos.

$$\Phi_{\text{C.L.}} = \frac{N_{\text{C.L.}}}{\epsilon \cdot \langle \sigma \rangle \cdot T \cdot N_p}$$

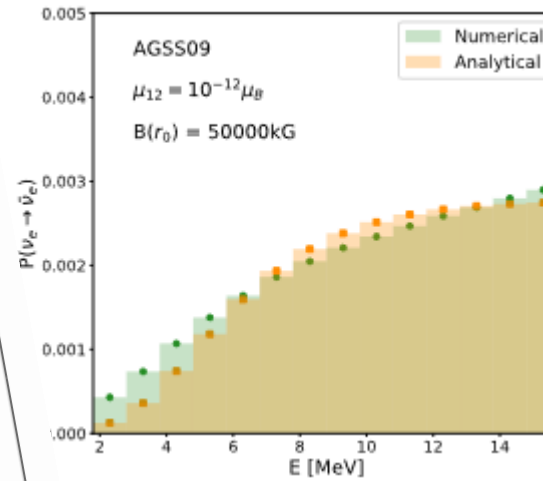
We provide the expected flux for different energy bins (and also the average probability).



USEFUL INFORMATION FOR FUTURE SEARCHES

E [MeV]	Numerical AGSS09		Analytical AGSS09	
	$\langle P_i \rangle$	$\langle \Phi_i \rangle [\text{cm}^{-2} \text{s}^{-1} \text{MeV}^{-1}]$	$\langle P_i \rangle$	$\langle \Phi_i \rangle [\text{cm}^{-2} \text{s}^{-1} \text{MeV}^{-1}]$
1.8 - 2.8	1.73×10^{-13}	4.62×10^{-8}	5.08×10^{-14}	1.36×10^{-8}
2.8 - 3.8	2.95×10^{-13}	1.18×10^{-7}	1.45×10^{-13}	5.82×10^{-8}
3.8 - 4.8	4.28×10^{-13}	2.24×10^{-7}	2.97×10^{-13}	1.55×10^{-7}
4.8 - 5.8	5.52×10^{-13}	3.34×10^{-7}	4.73×10^{-13}	2.86×10^{-7}
5.8 - 6.8	6.57×10^{-13}	4.19×10^{-7}	7.74×10^{-13}	4.07×10^{-7}
6.8 - 7.8	7.45×10^{-13}	4.62×10^{-7}	8.78×10^{-13}	4.80×10^{-7}
7.8 - 8.8	8.19×10^{-13}	4.55×10^{-7}	9.53×10^{-13}	4.88×10^{-7}
8.8 - 9.8	8.84×10^{-13}	4.03×10^{-7}	1.01×10^{-12}	4.35×10^{-7}
9.8 - 10.8	9.38×10^{-13}	3.15×10^{-7}	1.04×10^{-12}	3.38×10^{-7}
10.8 - 11.8	9.87×10^{-13}	2.11×10^{-7}	1.07×10^{-12}	2.23×10^{-7}
11.8 - 12.8	1.04×10^{-12}	1.12×10^{-7}	1.16×10^{-7}	
12.8 - 13.8	1.08×10^{-12}	3.87×10^{-8}	1.08×10^{-12}	3.89×10^{-8}
13.8 - 14.8	1.12×10^{-12}	5.77×10^{-9}	1.09×10^{-12}	5.63×10^{-9}
14.8 - 15.8	1.16×10^{-12}	2.83×10^{-10}	1.10×10^{-12}	2.68×10^{-10}

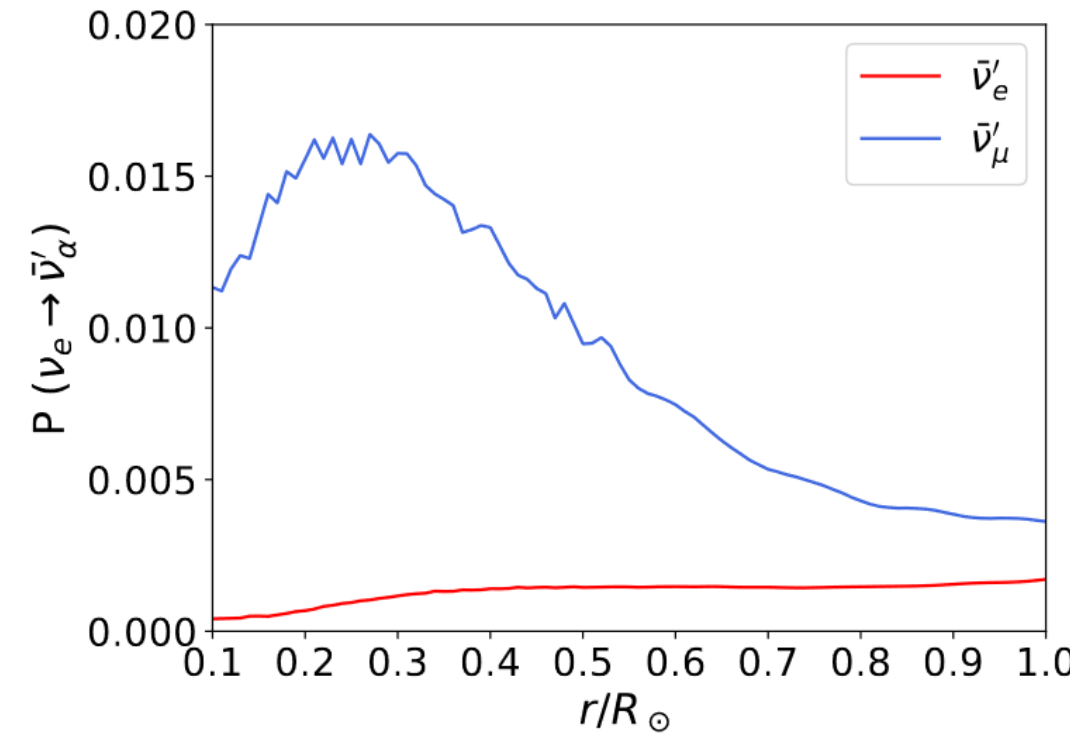
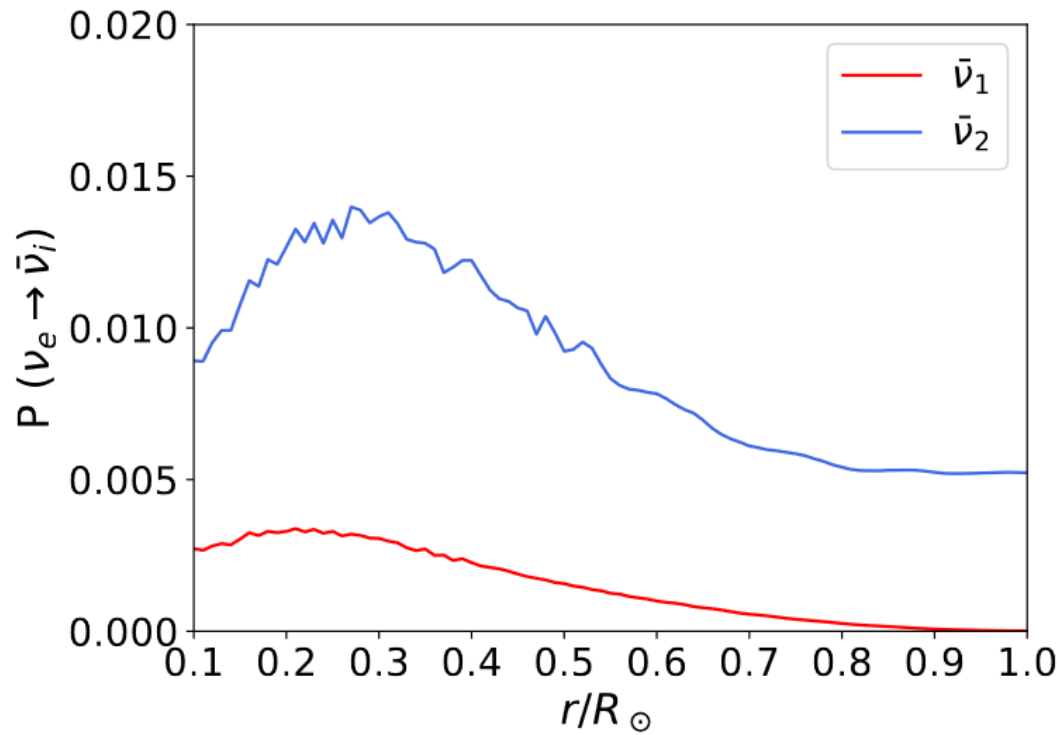
Table 1. Averaged $\bar{\nu}_e$ appearance probabilities and expected fluxes of $\bar{\nu}_e$ from the Sun for low-metallicity AGSS09 SSM. Detection through inverse beta decay is assumed; magnetic field profile (2.42) and $\mu_{12}B_\perp(r_0) = 10^{-12}\mu_B \cdot \text{kG}$ were chosen. For rescaling to different values of $\mu_{12}B_\perp(r_0)$ see text.



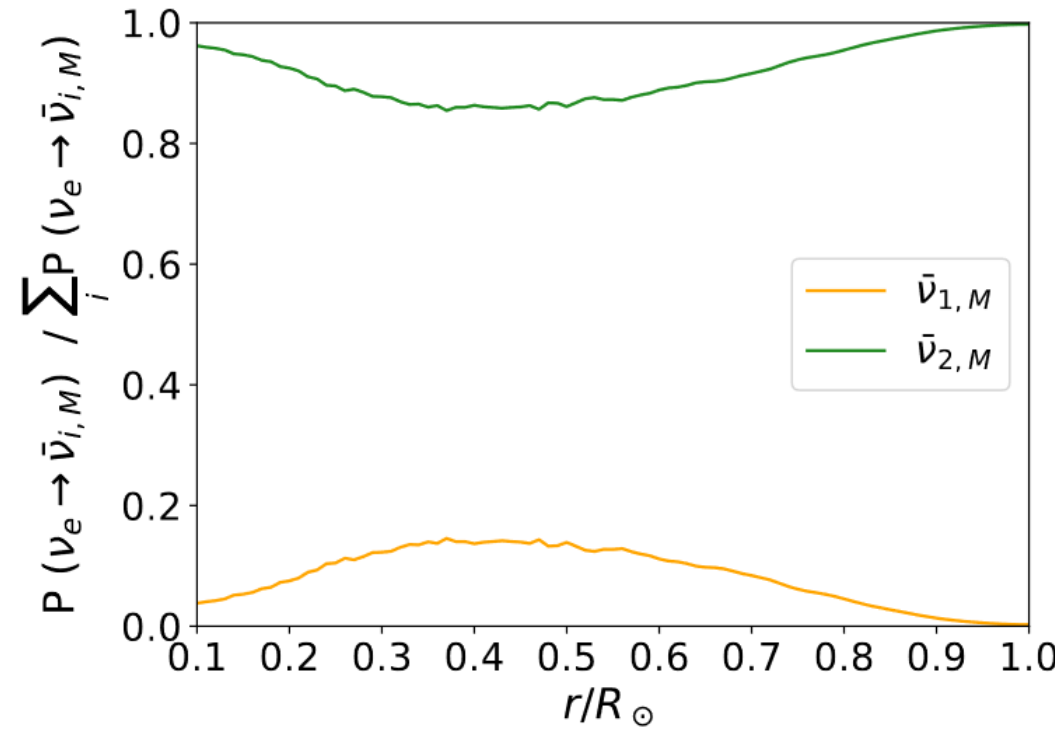
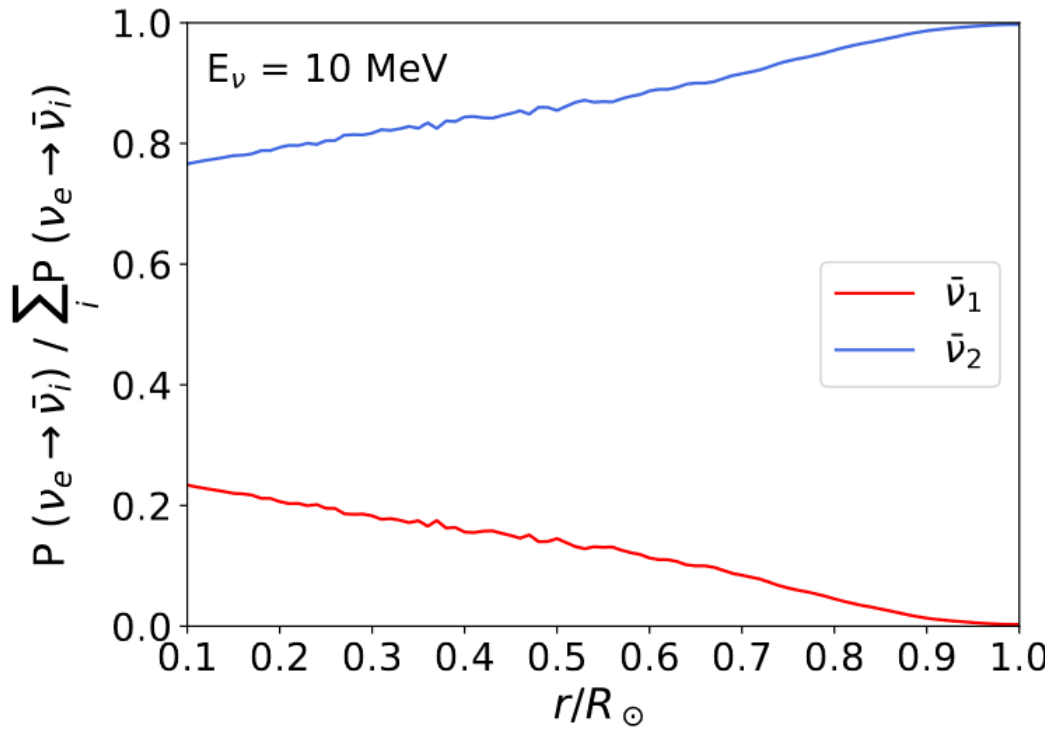
E [MeV]	Numerical GS98		Analytical GS98	
	$\langle P_i \rangle$	$\langle \Phi_i \rangle [\text{cm}^{-2} \text{s}^{-1} \text{MeV}^{-1}]$	$\langle P_i \rangle$	$\langle \Phi_i \rangle [\text{cm}^{-2} \text{s}^{-1} \text{MeV}^{-1}]$
1.8 - 2.8	2.03×10^{-13}	6.60×10^{-8}	5.43×10^{-14}	1.76×10^{-8}
2.8 - 3.8	3.43×10^{-13}	1.67×10^{-7}	1.55×10^{-13}	7.56×10^{-8}
3.8 - 4.8	4.92×10^{-13}	3.12×10^{-7}	3.19×10^{-13}	2.02×10^{-7}
4.8 - 5.8	6.27×10^{-13}	4.60×10^{-7}	5.06×10^{-13}	3.72×10^{-7}
5.8 - 6.8	7.41×10^{-13}	5.73×10^{-7}	6.82×10^{-13}	5.28×10^{-7}
6.8 - 7.8	8.39×10^{-13}	6.31×10^{-7}	9.35×10^{-13}	6.21×10^{-7}
7.8 - 8.8	9.23×10^{-13}	6.22×10^{-7}	1.0×10^{-12}	6.30×10^{-7}
8.8 - 9.8	9.96×10^{-13}	5.51×10^{-7}	1.07×10^{-12}	5.60×10^{-7}
9.8 - 10.8	1.06×10^{-12}	4.33×10^{-7}	1.10×10^{-12}	4.35×10^{-7}
10.8 - 11.8	1.12×10^{-12}	2.92×10^{-7}	1.13×10^{-12}	2.87×10^{-7}
11.8 - 12.8	1.18×10^{-12}	1.55×10^{-7}	1.14×10^{-12}	1.48×10^{-7}
12.8 - 13.8	1.24×10^{-12}	5.38×10^{-8}	1.15×10^{-12}	4.99×10^{-8}
13.8 - 14.8	1.29×10^{-12}	8.06×10^{-9}	1.16×10^{-12}	7.21×10^{-9}
14.8 - 15.8	1.34×10^{-12}	3.98×10^{-10}		3.43×10^{-10}

Table 2. Same as in Table 1 but for high metallicity GS98 SSM.

EVOLUTION INSIDE THE SUN



EVOLUTION INSIDE THE SUN



OTHER LIMITS

Experiment	Limit	Method
LAMPF	$\mu_{\nu_e} < 1.08 \times 10^{-9} \mu_B$ at 90% C.L.	Accelerator $\nu_e e^-$
LSND	$\mu_{\nu_e} < 1.1 \times 10^{-9} \mu_B$ at 90% C.L.	Accelerator $\nu_e e^-$
Krasnoyarsk	$\mu_{\nu_e} < 1.4 \times 10^{-10} \mu_B$ at 90% C.L.	Reactor $\bar{\nu}_e e^-$
ROVNO	$\mu_{\nu_e} < 1.9 \times 10^{-10} \mu_B$ at 95% C.L.	Reactor $\bar{\nu}_e e^-$
MUNU	$\mu_{\nu_e} < 9 \times 10^{-11} \mu_B$ at 90% C.L.	Reactor $\bar{\nu}_e e^-$
TEXONO	$\mu_{\nu_e} < 7.4 \times 10^{-11} \mu_B$ at 90% C.L.	Reactor $\bar{\nu}_e e^-$
GEMMA	$\mu_{\nu_e} < 2.9 \times 10^{-11} \mu_B$ at 90% C.L.	Reactor $\bar{\nu}_e e^-$
CONUS	$\mu_{\nu_e} < 7.5 \times 10^{-11} \mu_B$ at 90% C.L.	Reactor CE ν NS
Dresden-II	$\mu_{\nu_e} < 2.2 \times 10^{-10} \mu_B$ at 90% C.L.	Reactor CE ν NS
LAMPF	$\mu_{\nu_\mu} < 7.4 \times 10^{-10} \mu_B$ at 90% C.L.	Accelerator $\nu_\mu e^-$
BNL-E-0734	$\mu_{\nu_\mu} < 8.5 \times 10^{-10} \mu_B$ at 90% C.L.	Accelerator $\nu_\mu e^-$
LSND	$\mu_{\nu_\mu} < 6.8 \times 10^{-10} \mu_B$ at 90% C.L.	Accelerator $\nu_\mu e^-$
DONUT	$\mu_{\nu_\tau} < 3.9 \times 10^{-7} \mu_B$ at 90% C.L.	Accelerator $\nu_\tau e^-$



OTHER LIMITS



Experiment	Limit at 90%C.L.	Energy range
Borexino	$\mu_{\nu\text{SOLAR}} < 2.8 \times 10^{-11} \mu_B$	0.19 MeV – 2.93 MeV
Super-Kamiokande	$\mu_{\nu\text{SOLAR}} < 1.1 \times 10^{-10} \mu_B$	5 MeV – 20 MeV
LUX-ZEPLIN	$\mu_{\nu\text{SOLAR}} < 6.2 \times 10^{-12} \mu_B$	$E \leq 2 \text{ MeV}$
XENONnT	$\mu_{\nu\text{SOLAR}} < 6.3 \times 10^{-12} \mu_B$	$E \leq 1 \text{ MeV}$

OTHER LIMITS



Limit	Method
$\mu_{\nu\text{PLASMON}} < 1.2 \times 10^{-12} \mu_B$ at 95% C.L.	Tip of red-giant branch
$\mu_{\nu\text{PLASMON}} < 1.0 \times 10^{-11} \mu_B$ at 95% C.L.	Pulsating white dwarfs
$\mu_{\nu\text{PLASMON}} < 2.2 \times 10^{-12} \mu_B$ at 95% C.L.	Luminosity
$\mu_{\nu\text{PLASMON}} < 2.2 \times 10^{-12} \mu_B$ at 95% C.L.	Luminosity

OTHER LIMITS



Limit	Method
$\mu_{\nu\text{PLASMON}} < 1.2 \times 10^{-12} \mu_B$ at 95% C.L.	Tip of red-giant branch
$\mu_{\nu\text{PLASMON}} < 1.0 \times 10^{-11} \mu_B$ at 95% C.L.	Pulsating white dwarfs
$\mu_{\nu\text{PLASMON}} < 2.2 \times 10^{-12} \mu_B$ at 95% C.L.	Luminosity
$\mu_{\nu\text{PLASMON}} < 2.2 \times 10^{-12} \mu_B$ at 95% C.L.	Luminosity

OTHER LIMITS



Limit	Method
$\mu_{\nu\text{PLASMON}} < 1.2 \times 10^{-12} \mu_B$ at 95% C.L.	Tip of red-giant branch
$\mu_{\nu\text{PLASMON}} < 1.0 \times 10^{-11} \mu_B$ at 95% C.L.	Pulsating white dwarfs
$\mu_{\nu\text{PLASMON}} < 2.2 \times 10^{-12} \mu_B$ at 95% C.L.	Luminosity
$\mu_{\nu\text{PLASMON}} < 2.2 \times 10^{-12} \mu_B$ at 95% C.L.	Luminosity

NEUTRINO EVOLUTION IN THE SUN

In the primed basis,

$$\mu_{e'\mu'} = \mu_{12} e^{-i\lambda_2},$$

$$\mu_{e'\tau'} = \left(\mu_{13} c_{12} + \mu_{23} s_{12} e^{-i\lambda_2} \right) e^{-i(\lambda_3 - \delta_{\text{CP}})}$$

$$\mu_{\mu'\tau'} = \left(\mu_{23} c_{12} e^{-i\lambda_2} - \mu_{13} s_{12} \right) e^{-i(\lambda_3 - \delta_{\text{CP}})}$$

$$U = O_{23} \Gamma_\delta O_{13} \Gamma_\delta^\dagger O_{12} \quad U_M = UK \quad K = \text{diag}(1, e^{i\lambda_2}, e^{i\lambda_3})$$

ELECTRON ANTINEUTRINO APPEARANCE PROBABILITY

Simplified version for energies $E > 5$ MeV

$$P(\nu_{eL} \rightarrow \bar{\nu}_{eR})_{\text{simpl.}} = \frac{1}{2} c_{13}^4 \sin^2 2\theta_{12} B_{\perp}^2(r_0) |\mu_{12}|^2 \left(\frac{\sin^2 \tilde{\theta}(r_0)}{g'_2(r_0)} \right)^2$$

Or even simpler!

$$P(\nu_{eL} \rightarrow \bar{\nu}_{eR}) \simeq 1.1 \times 10^{-10} \left(\frac{\mu_{12} B_{\perp}(r_0)}{10^{-12} \mu_B \cdot 10 \text{ kG}} \right)^2$$

ATTENTION: not valid for experiments sensitive to pp, pep and ${}^7\text{Be}$ neutrinos